MSE 464 Simulation Project 3: Domains

Jacob Christensen, Stasiu Chyczewski, Michael Coppedge

Introduction

Magnetic domains are a key feature of most magnetic systems, serving to reduce magneto-static energy as well as playing a large part in magnetization reversal. Domains can be studied to learn more about material properties (e.g. Dzyaloshinskii-Moriya interaction) and understand magnetization reversal in a sample. Beyond physical curiosity domains are also of interest in magnetic device applications, particularly magnetic racetrack memory. In order to use domains for these purposes however, the basics of how they behave must first be understood. In this project, we simulate basic domain wall statics, motion, and pinning to develop an intuition of how this critical magnetic phenomenon behaves. The systems described and studied in this report were modeled using the Ubermag Python package (https://ubermag.github.io/index.html) with OOMMF as a backend.

Part 1: Domain Wall Statics (lead: Michael)

We begin this study of micromagnetic simulations of domain walls by first initializing and visualizing domain walls under static conditions. In this section, the effects of the inclusion or exclusion of different energy terms on the domain walls are investigated.

The system is a rectangular prism with dimensions 500 nm x 20 nm x 2.5 nm (length x width x height/thickness; X x Y x Z). It is discretized into cubic cells with side lengths of 2.5 nm, reducing its dimensions in cell units to 200 x 8 x 1, essentially making it a long, thin film or strip. It is given initial material parameters similar in magnitude to those of permalloy - these parameters being the saturation magnetization, $M_s = 5.8 \times 10^5$ A/m, and the exchange energy constant, A = 13 pJ/m. Other parameters, such as uniaxial anisotropy, will be introduced and explored later in this section.

As an initial test, a two domain configuration is initialized with its wall in the middle of the strip. Moments to the left of the wall are pointed uniformly in the +x direction, and to the right of the wall pointed uniformly in the –x direction; that is, they are pointed towards each other – towards the center of the strip. Only the exchange and demagnetization energies are considered at this stage, giving this system an energy equation as follows:

$$-A\mathbf{m} \cdot \nabla^2\mathbf{m} - \tfrac{1}{2}\mu_0 M_s \mathbf{m} \cdot \mathbf{H}_d$$

Relaxing the system results in the configuration of moments in the domain wall region shown in figure I-1.

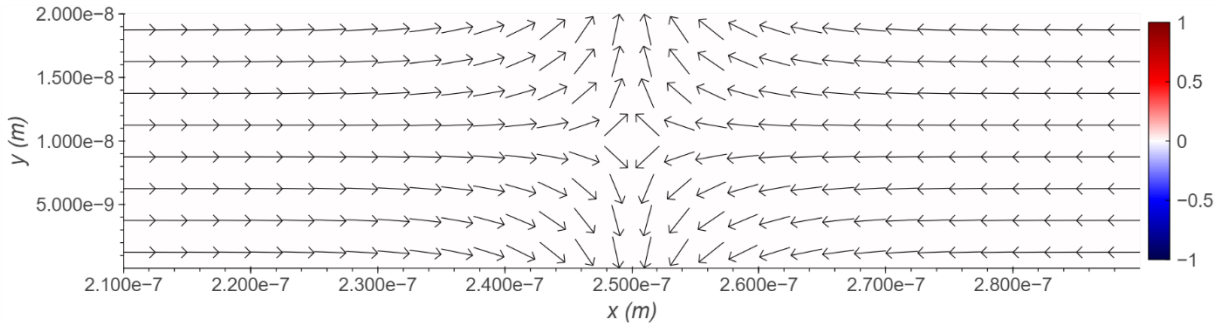

Figure I-1: Incoherent spin orientations in the domain wall region of the first system, defined by two initial domains, each 250 nm wide, pointing in the +x and –x directions.

Note that this figure, and all subsequent figures in this section are top-down visualizations of the system. Because it is only 1 cell thick in the z-direction, this visualization captures much of the relevant information about the orientation of the spins in the domain wall. Additionally, the colorbar indicates the out-of-plane component of the spins while the length of the vector arrow indicates its in-plane magnitude; thus, in this first case, the spins remain entirely in plane even after relaxation. However, the spins do not rotate coherently in the domain wall region. We can alter this observed behavior by initializing a third, 10 nm wide domain pointing in either the +y or –y direction between the larger, outer two domains (Figures I-2a and I-2b). (Figures I-2a and I-2b).

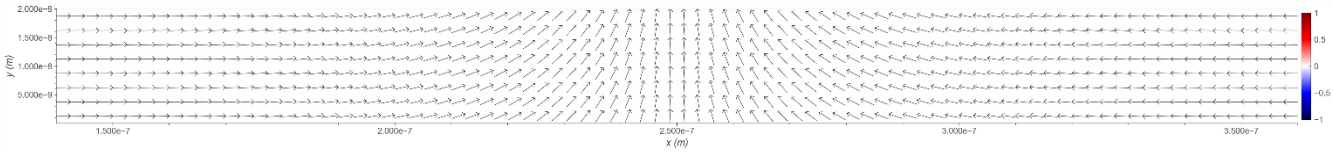

Figure I-2a: Coherent spin orientations in the domain wall of the system are achieved when it is initialized with a third, 10 nm wide domain pointing in the +y direction, placed between the two outer domains.

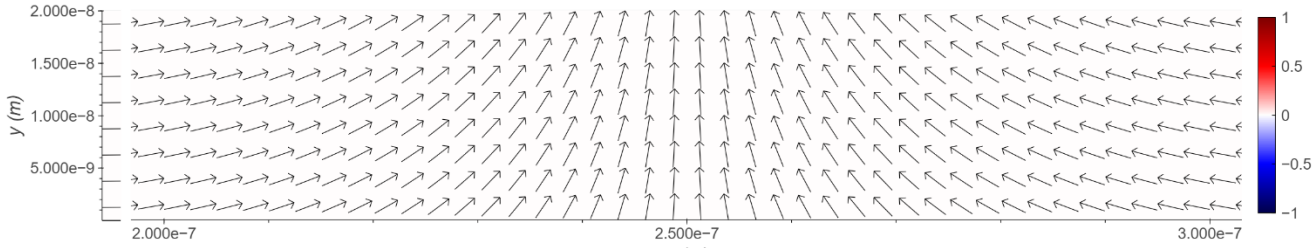

Figure I-2b: A zoomed in version of Figure I-2a, showing nearly the full width of the domain wall.

The above domain wall is wide – at least 100 nm wide (as seen in Figure I-2b), which accounts for over 20% of the entire system's length. By introducing a third term to the energy equation, a uniaxial anisotropy in the x-direction, we can shrink the domain wall. We use an anisotropy constant of $K_u = 0.5 \times 10^6$ J/m^3. Using the same initial three domain configuration as that which was just described, although now with x-direction anisotropy, we obtain the domain wall as shown below.

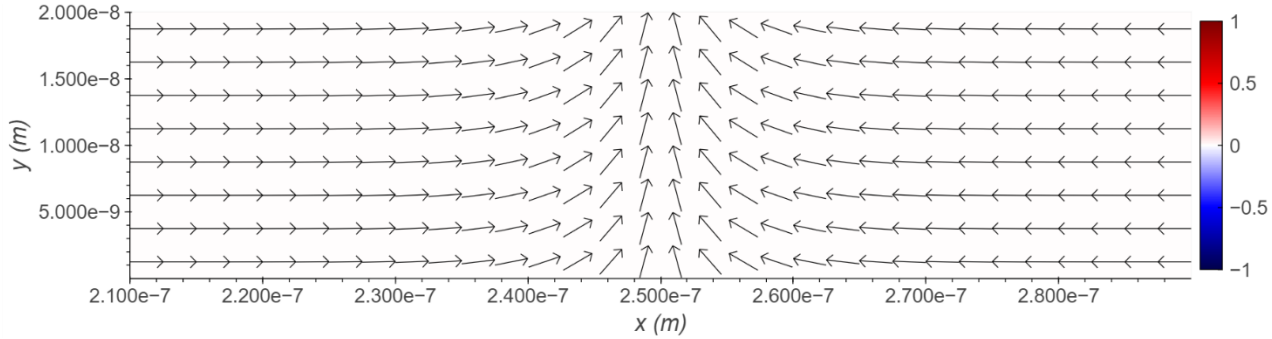

Figure I-3: The domain wall of the same initial system that was described in Figures I-2a and I-2b, although with x-direction uniaxial anisotropy.

This domain wall is not as wide as that which was observed in the system that was without anisotropy – this is the expected behavior. The anisotropy energy is minimized when the moments are aligned with the easy axis, and maximized when they orient in a perpendicular direction. In the preceding case, the domain wall was wide and many spins had y-direction components because that was favorable for the exchange energy – gradual rotation of the spins over a long distance is preferable as nearest neighbors are more parallelly aligned. However, with both energy terms it becomes a competition between gradual rotation to minimize exchange and rapid rotation to minimize anisotropy energy. Consequently, by introducing an anisotropy, the domain wall would have a greater energy if it were to retain the previous spin configurations. This is reflected in the equation typically used for calculating domain wall widths:

$$\delta_w = \pi \left(\frac{A}{k}\right)^{\frac{1}{2}}$$

Stronger exchange coupling causes domain walls to be wider, just as stronger anisotropy forces them to be smaller. In the case of the material defined here, it is clear that the anisotropy is strong enough to play a significant role in shrinking the domain.

For the next system, we consider initial domains pointing in the +y and –y directions. Analogous to the observations made with the previous system, incoherent rotation in the domain wall region is obtained without a third domain initialized between the outer two.

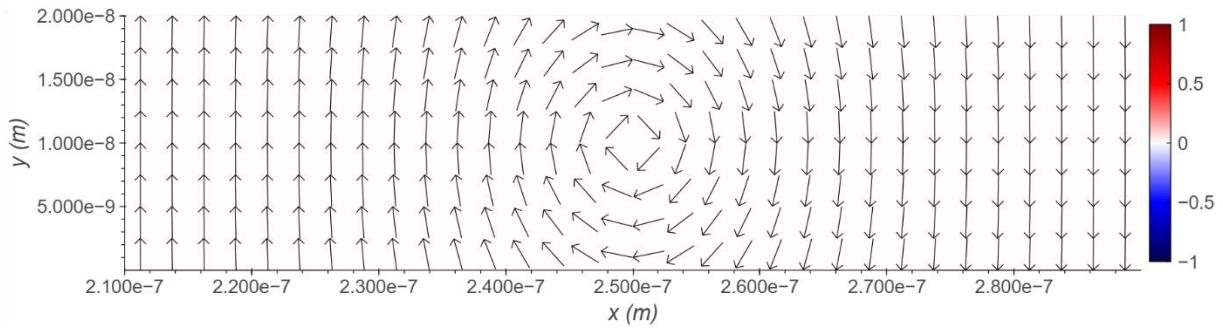

Figure I-4a: Incoherent spin orientations in the domain wall region of the second system, defined by two initial domains, each 250 nm wide, pointing in the +y and –y directions. This system has no uniaxial anisotropy.

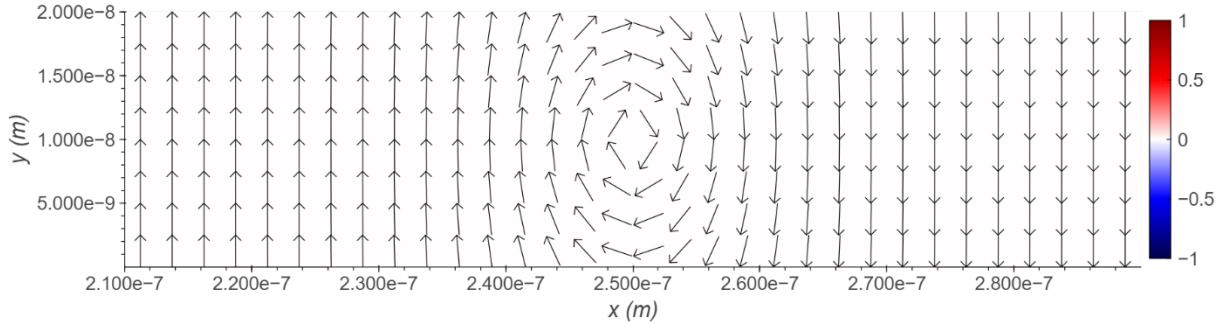

Figure I-4b: Incoherent spin orientations in the domain wall region of the second system, defined by two initial domains, each 250 nm wide, pointing in the +y and –y directions. This system has uniaxial anisotropy in the y-direction.

Note that we can indeed initialize two oppositely aligned y-direction domains without anisotropy (Figure I-4a), and that the introduction of y-direction anisotropy ($K_u = 0.5x10^6$ J/m^3) serves only to shrink the incoherent domain region slightly (Figure I-4b), for those same reasons explained in the preceding discussion of the first system. As before, an additional, third domain is required in the initialization to obtain coherent rotation (Figure I-5a).

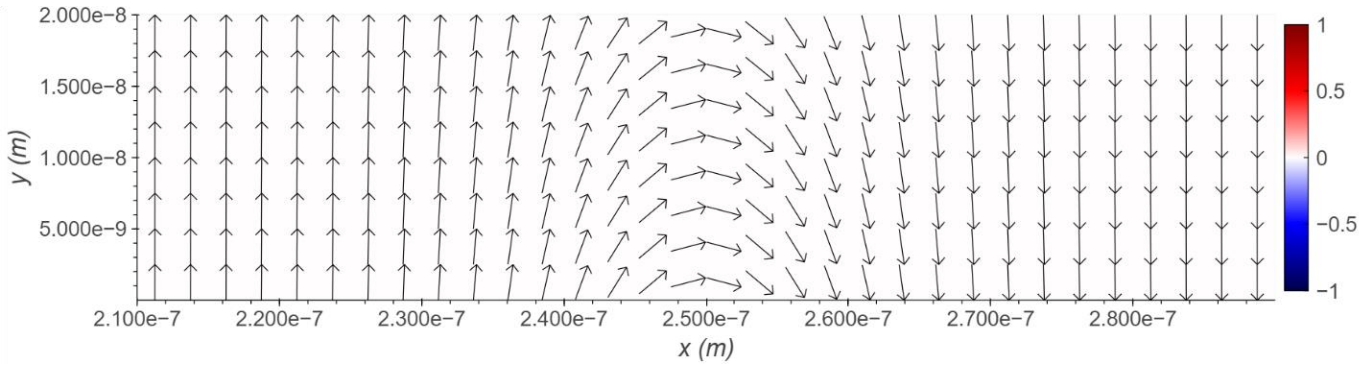

Figure I-5a: Coherent spin orientations in the domain wall of the second system are achieved similarly to the first – with the inclusion of a third, 10 nm wide domain pointing in a perpendicular direction to the outer two. In this case, the +x direction was selected. This system shown has uniaxial anisotropy in the y-direction.

Decreasing the anisotropy constant used for this coherent example performs as expected by increasing the length of the domain wall (Figure I-5b). The reason here is the same as has been previously explained.

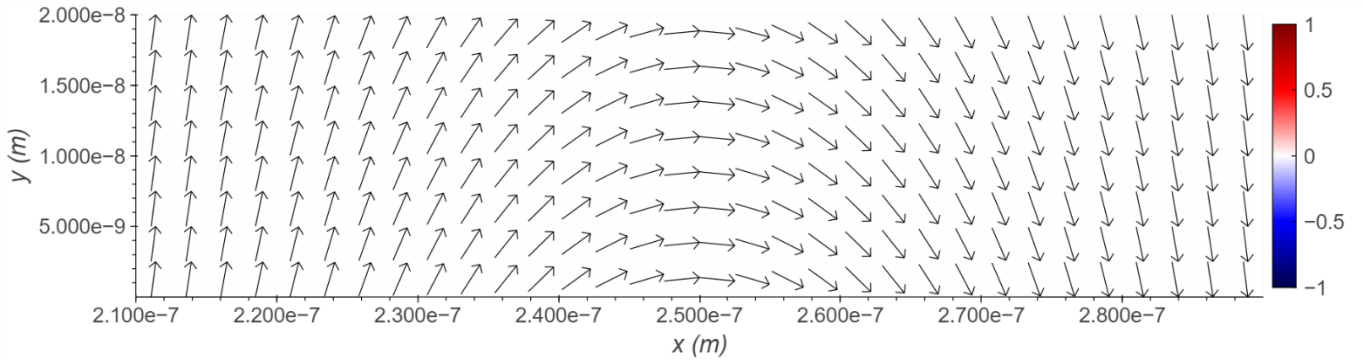

Figure I-5b: Coherent spin orientations in the domain wall of the second system. With a decreased anisotropy constant relative to the system visualized in Figure I-5a, the domain wall widens.

Out-of-plane magnetizations differ, however. When attempting to initialize two domains, one pointing in the +z and one in the –z direction, anisotropy must be included, else the system will relax to a state that does not resemble the initial domain definitions.

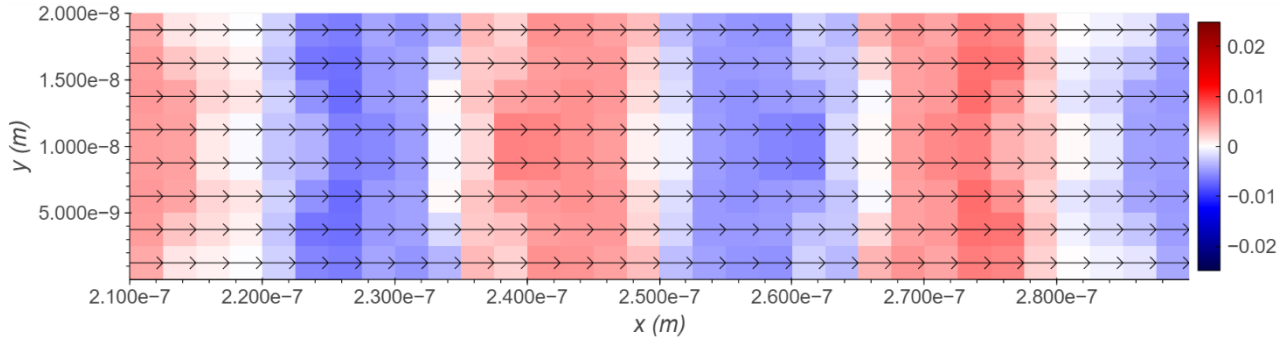

Figure I-6: Domains cannot be initialized properly with out-of-plane orientations without z-direction anisotropy.

In the above example (Figure I-6), the two initial z-oriented domains collapse back in plane, albeit with seemingly random, very slight out-of-plane canting. Although we do not have a working explanation for this canting behavior (and, in particular, why it seems to oscillate into and out of the plane of the system), the reason the system cannot retain z-oriented moments without anisotropy is because there are significantly more surface magnetic charges in this case – the z-plane surfaces of the system have areas 8 times greater than the y-plane surfaces. The demagnetizing energy is simply too large for the system to be able to retain the domains we specified, and so it collapses back in-plane. Z-direction anisotropy must be included to provide a sufficient energetic favorability to allow the moments to persist in an out-of-plane orientation. Using a similar three domain configuration as has been used for the previous systems, as well as a z-direction uniaxial anisotropy ($K_u = 0.5x10^6$ J/m^3), the following domain walls are obtained:

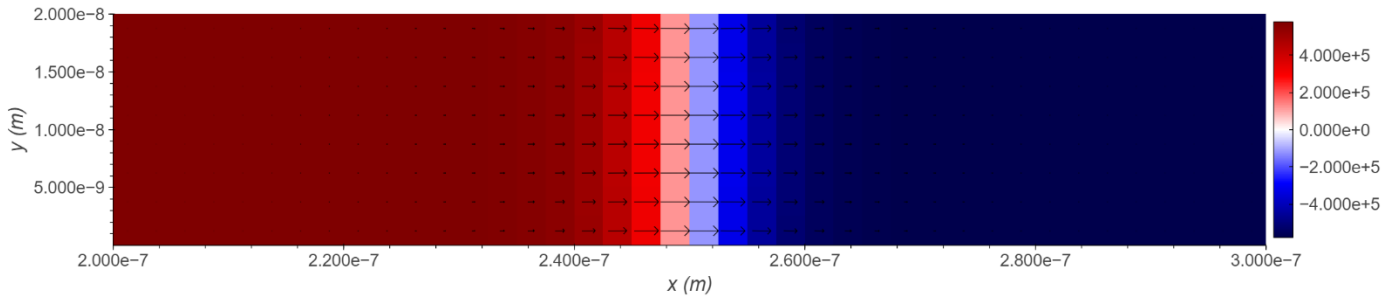

Figure I-7a: Out-of-plane domains can persist with the addition of z-direction anisotropy. Here, the third, 10 nm wide domain is initialized in the +x direction.

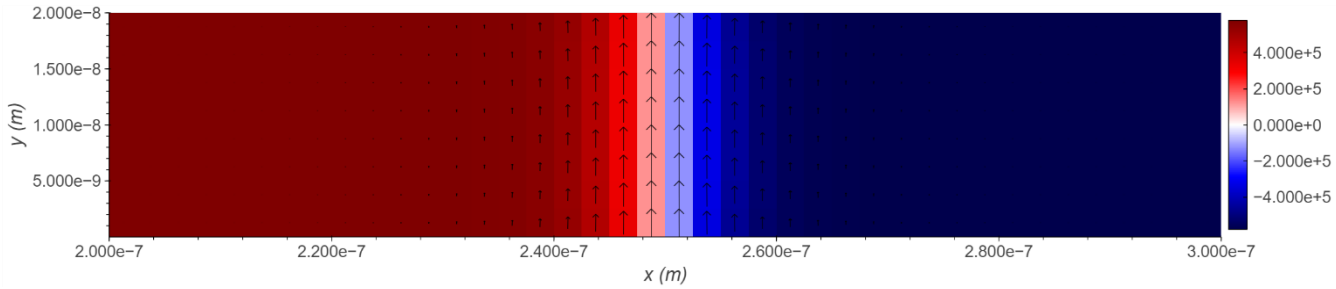

Figure I-7b: Out-of-plane domains can persist with the addition of z-direction anisotropy. Here, the third, 10 nm wide domain is initialized in the +y direction.

In the case where the third domain is initialized in the x-direction (Figure I-7a), the moments rotate perpendicularly relative to the plane of the domain wall – thus, this is a Néel wall. In the

opposite case, where the third domain is y-oriented, the moments rotate parallel relative to the domain wall plane, giving a Bloch wall.

The final investigations of this section involve eliminating the need for the manual initialization of a small, third domain to obtain coherent rotation over the domain wall. To do so, we introduce a fourth and final term to the system's energy equation, the Dzyaloshinskii-Moriya interaction (DMI). Unlike regular exchange, the DMI prefers perpendicular alignment of neighboring spins (note that the DMI also requires specification of a crystal class. We use Cnv_z, which is typically more applicable to thin film type systems compared to the other available crystal classes). Including all terms thus far introduced, the energy equation of the system becomes:neighboring spins (note that the DMI also requires specification of a crystal class. We use Cnv_z, which is typically more applicable to thin film type systems compared to the other available crystal classes). Including all terms thus far introduced, the energy equation of the system becomes:

$$-A\mathbf{m}\cdot\nabla^2\mathbf{m} - \tfrac{1}{2}\mu_0 M_s\mathbf{m}\cdot\mathbf{H}_d - K(\mathbf{m}\cdot\mathbf{u})^2 + D(\mathbf{m}\cdot\nabla m_z - m_z\nabla\cdot\mathbf{m})$$

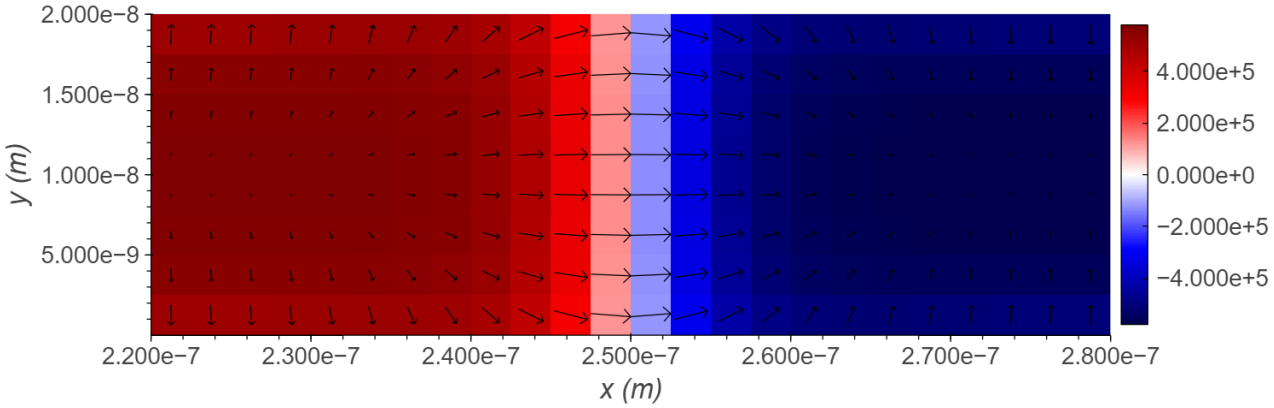

Figure I-8: Coherent domain walls can be obtained without a manually specified third domain with the addition of the DMI energy term. Here, the uniaxial anisotropy is in the z-direction.

In the above example (Figure I-8), two domains are initialized, one in the +z and the other in the –z direction. Despite this, a coherent domain wall is obtained even without manual inclusion of a third initial domain. Additionally, the system relaxes to a state in which the domain wall is of the Néel type. This is consistent with what we have discussed in lecture, where thinner films prefer Néel walls. The Coey textbook also mentions that Néel type walls are only stable in thin films where the width of the wall is greater than the thickness of the film. In this case we see that the wall spans approximately 10-20 cell units – this is much greater than the system's thickness of only 1 cell unit.

Finally, we demonstrate that, in order to initialize and retain a domain wall that is not located at the center of the strip, the demagnetization energy must be neglected. Thus far, it has been the case for every system described that the domain wall was centralized. Excluding demagnetization effects and retaining the other three energy terms results in the following state:

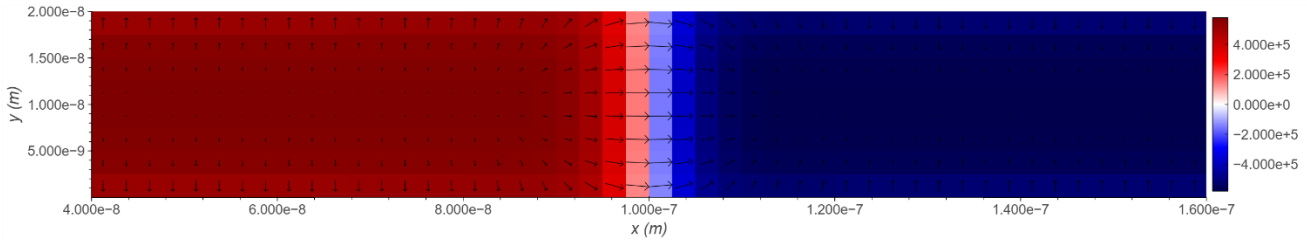

Figure I-9: Domain walls can be initialized elsewhere in the system by neglecting the demagnetization energy.

Although this is visually similar to Figure I-8, note that the domain wall is centered at 100 nm, instead of 250 nm. This is important for subsequent sections of the project, in which domains will be initialized on one side of the strip and then driven across to the other side. Interestingly, there exists a somewhat predictable relationship between the initial location of the domain wall and the time it takes for the relaxation computation to be performed.

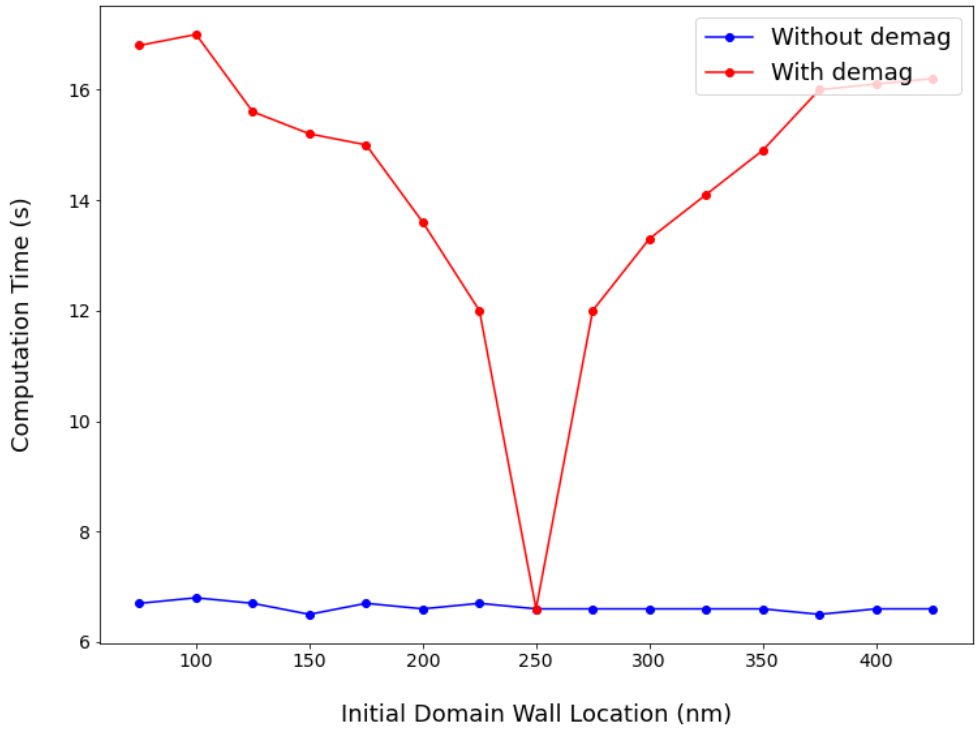

Figure I-10: Computation time (as performed on the author's personal laptop computer) as a function of the location of the initial domain wall, based on whether or not the demagnetization energy term was included. 250 nm is the center of the system.

As can be seen above, the calculation takes longer to preform when the initial domain wall is placed further from the center of the system when demagnetization is included. Because the wall always minimizes to the center of the system when demagnetization is included, we even see that the computation time drops to that of the system that does not account for demagnetization, when the wall is already placed at the center of the system.

Part 2: Domain Wall Motion (lead: Stasiu)

Unsurprisingly, domain walls can coherently move as a function of time. Potential means of controllably moving domain walls include the use of an external field (i.e. Zeeman energy) and through the use of a spin-polarized current (spin-transfer torque). The deterministic control of domain wall motion is of interest in device engineering applications, particularly memory devices in the form of magnetic racetrack memory. In this section we demonstrate the motion of domain wall by these mechanisms as well as the velocity breakdown that can happen at high applied field (Walker breakdown).

We start by creating a 500 nm x 200 nm x 2.5 nm strip with a cubic cell size of 2.5 nm per side and material parameters meant to approximate permalloy as done in the preceding section. Two domain walls are initialized by defining a positively magnetized (z-direction) region from x = 20 nm to x = 40 nm against a negatively magnetized background and then relaxing the system. For this simulation we only consider the exchange, uniaxial anisotropy (z-direction), and DMI energy terms. We neglect demagnetizing fields. This initialized state is shown below in Fig. II-1.

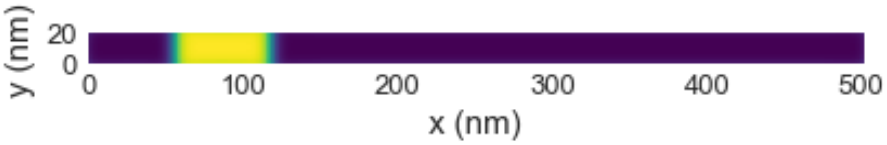

Figure II-1: Initial state after relaxation. Note that the color scale shows magnetization in the z-direction, with yellow being positive saturation and purple being negative saturation.

We first study the effect of an applied field by introducing the Zeeman term ($\mu_0 \boldsymbol{M}_s \mathbf{m} \cdot \mathbf{H}$) to the system's energy. Upon applying a field of -10 kA/m in the -z direction and driving the system for 5 ns, we can see that the domain walls have both moved inwards (i.e., opposite directions) as shown in Fig. II-2.

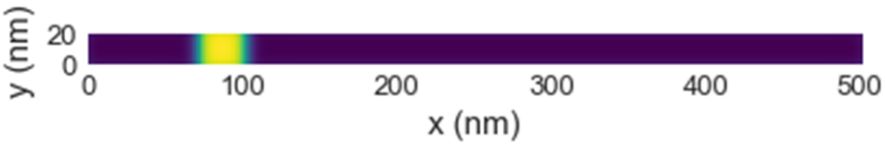

Figure II-2: System in the presence of a 10 kA/m magnetic field in the -z direction

The applied field exerts pressure on the walls, pushing them together. This can be intuitively thought of as the strip beginning to full magnetize itself to align with the applied field, destroying the positively magnetized region. Consequently, the domain walls do not move together, but instead oppose each other.

We next study the effect of an applied current in the system. A spin polarized current can exert a torque on a magnetized layer via angular momentum transfer from inject spin polarized electrons. In real devices, a spin-polarized current is typically created by injecting a charge current into a ferromagnet. This spin-transfer torque (STT) can be much stronger than the that from an applied external field. To simulate this, we add the Slonczewski term ($\gamma_0 \beta \epsilon \left(\mathbf{m} \times \mathbf{m}_\mathrm{p} \times \mathbf{m}\right) - \gamma_0 \beta \epsilon' \left(\mathbf{m} \times \mathbf{m}_\mathrm{p}\right)$) to the system's dynamics (and removing the Zeeman term from the energy expression). We set $\Lambda = 2$, $J = 1 * 10^{12}$ A/m^2, spin current in y-direction, and $P = 0.4$. After driving the initial system with these conditions for 0.5 ns, we can see that the domain walls have moved together as shown in Fig. II-3.

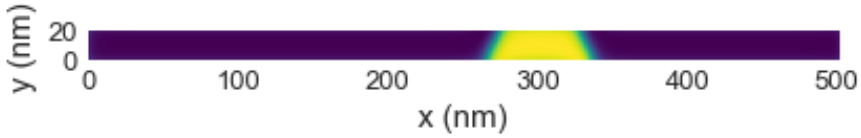

Figure II-3: System driven with spin polarized current

As expected, the domain walls move much faster in the presence of a strongly spin polarized current instead of a field (note that the simulation time differs by a factor of 10). Unlike the domain wall motion from the Zeeman energy, the domain walls here also move together in the same direction while roughly preserving the size of the positively magnetized region. The domain walls themselves are also no longer perfectly aligned in the y-direction, tilting slightly from the torque.

We repeat the above tests for strips with a single domain wall. The initial state, results for the Zeeman energy driven motion and current driven motion are shown in Fig. II-4. The results are very similar to those for the dual domain walls, with current driven motion being much faster than field driven motion.

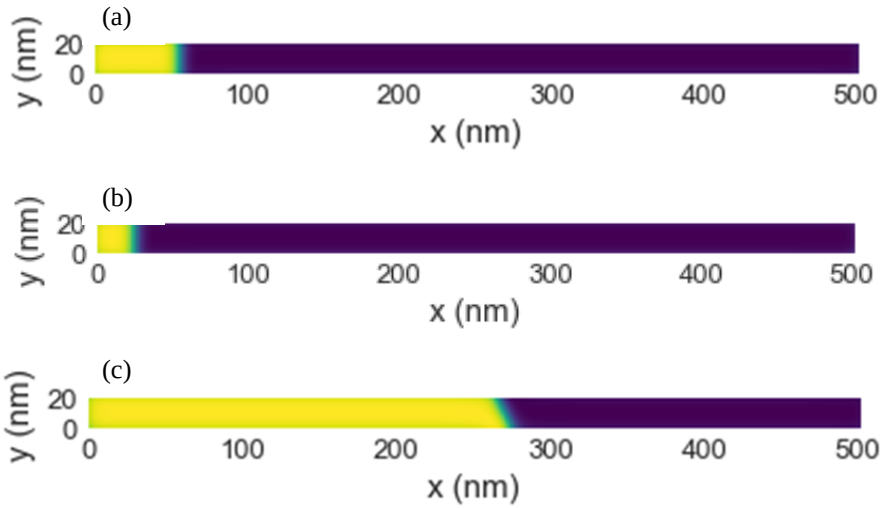

Figure II-4: Single domain wall simulations. (a) Initial state (b) field-driven motion (c) current-driven motion

We next simulate the Walker breakdown of domain wall velocity. As domain walls move in an applied perpendicular field, the spins in the wall precess. As the field (and by extension) domain wall velocity increase, the angular velocity of these precessions approach the ferromagnetic resonance frequency of the material. This results in walker breakdown, which can be seen as a sudden drop in the average domain wall velocity as a function of applied field. We study this here by considering a 4.4 μm x 100 nm x 5 nm magnetic strip with a cubic cell size of 5 nm per side. Here, we consider only the exchange energy and shape anisotropy in the system's energy. We initialize the strip with a domain wall pointing in the y direction in the middle of the strip. The magnetization is in the positive and negative x direction on either side as shown in Fig. II-5.

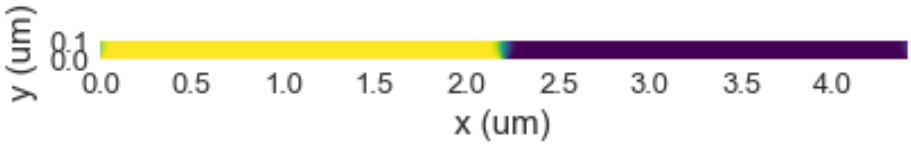

Figure II-5: Initialized state for walker breakdown simulation

Next, we various fields in the positive x-direction and drive the simulation for 2 ns. We apply fields in 5 Oe increments up to 60 Oe and calculate the average velocity dividing the displacement of the domain wall by simulation time. Fig. II-6 shows the average velocity vs. applied field for this range. A higher resolution scan was complicated by the simulation time.

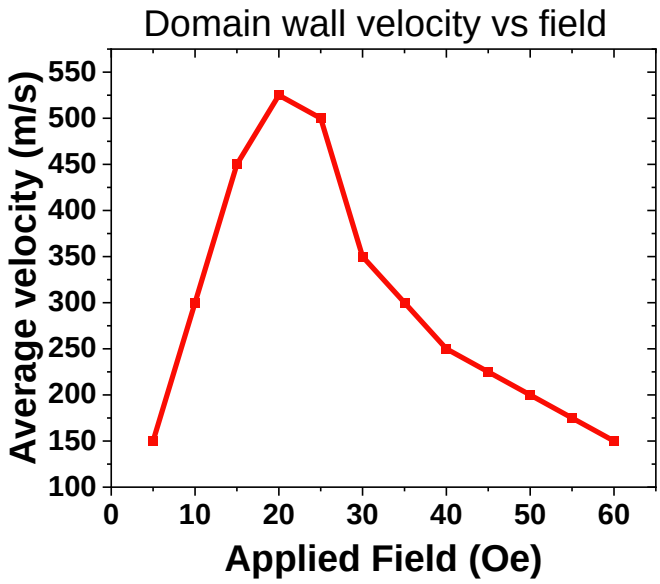

Figure II-6: Average domain wall velocity vs. applied field

After the range plotted above, the domain wall velocity begins to slowly fall before sharply rising and starting to oscillate. This is apparent in the oscillating end points of the domain wall in each simulation. In addition, the domain wall loses its clean vertical shape, rotating/becoming irregularly shaped. Fig. II-7. shows this behavior in fields from 150-170 Oe. At a field of about 300 Oe, the strip saturates within the 2 ns simulation period.

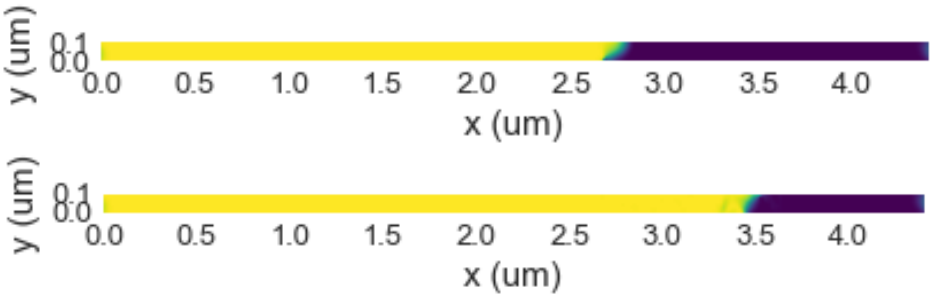

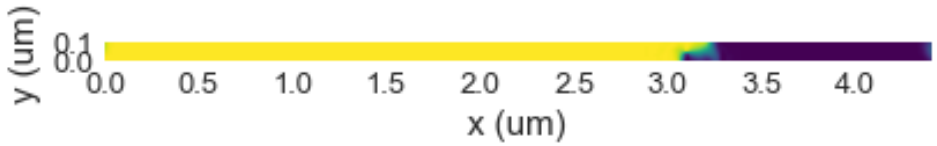

Figure II-7: Final domain wall position at fields of 150 Oe, 160 Oe, and 170 Oe from top to bottom.

Part 3: Domain Wall Pinning (lead: Jacob)

Defects in a magnetic material can change the motion of a domain wall when a magnetic field is applied. The domain wall energy per unit area is given by $\gamma_w = 4\sqrt{AK}$, where A is the exchange constant and K is the anisotropy constant. When a defect in a magnetic material has values of A or K which differs from the bulk values, the defect can pin a domain wall which moves across it. This effect is especially pronounced for void defects, when $A = 0$ and $K = 0$. Additionally, larger defects will more easily pin a domain wall. In this part of the project, we experiment with void defects in the form of notches created in the sides of our magnetic strip.

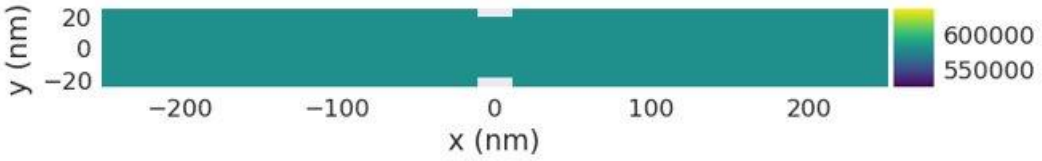

Figure III-1: Magnetic strip of 200 nm length, 50 nm width, and 1 cell thickness. Two notches have been created in the center of the film, each 20 nm in length and 5 nm deep. The film currently only has one magnetic domain.

We start by creating the magnetic strip with a 200 nm length, 50 nm width, and 1 cell thickness. Then we create two notches of 5 nm depth and 20 nm length on either side of the film, as seen in Fig. III-1. We split the strip into two domains with a single domain wall 50 nm from the left side of the strip, where the domains have magnetization pointing in opposite directions along the z-axis. Minimizing this configuration results in an increase in the size of the domain wall length δ_w, as seen in Fig. III-2. This result is expected because the new configuration decreases the energy penalty for flipping the moments from one domain to the next. Recall that domain wall width is determined by the balance between exchange energy and magnetic anisotropy. Because the exchange term seeks to have the smoothest possible variation in magnetization direction, we have a prohibitively large exchange energy penalty when the spins flip instantly like in the configuration before minimization. Therefore, upon minimizing the energy, δ_w increases so that the spins can flip from one domain to the next more gradually. The wall does not have infinite width, though, as this would incur a large penalty from the anisotropy energy.

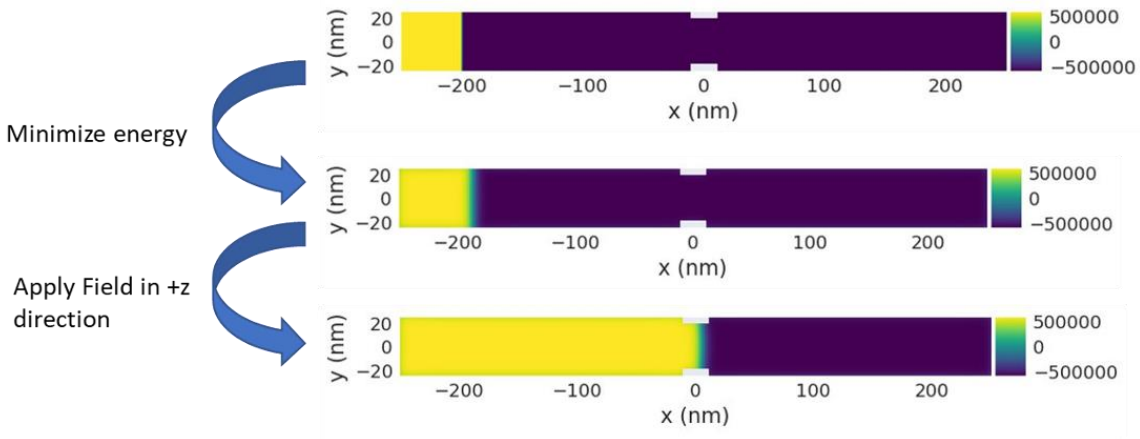

Figure III-2: The magnetic strip is first made to have two domains separated by a wall 50 nm from the left side of the film (top plot). Upon minimizing the energy, the wall's length increases (middle plot). Finally, applying a magnetic field in the +z direction pins the wall to the notches (bottom plot).

A magnetic field introduced into the system will apply a pressure to the domain wall. Because the domain wall has a Zeeman energy per unit area of $2\mu_0 MH\delta x$ when in an applied field H , the pressure exerted on the wall by the field will be $2\mu_0 MH$. In our case, we apply a field in the +z direction, which then exerts a pressure in the +x direction. A relatively smaller field will be unable to move the wall past the notches, ending with the wall pinned by the defects (Fig. III-2). However, if a strong enough field is applied the wall can move past the notches and make it to the right end of the strip. With trial and error, it was found that a minimum field of approximately $H = 1.16515 * 10^5$ A/m was needed to drive the wall all the way across the strip (Fig. III-3).

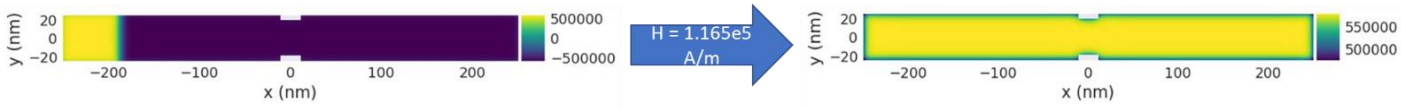

*Figure III-3: Applying a minimum field of H = 1.16515 * 10^5 A/m results in the wall being pushed to the end of the film with 5 nm depth notches.*

For these magnetic simulations we included the anisotropy energy, exchange energy, Dzyaloshinskii-Moriya energy, and when applicable, the Zeeman energy. The demagnetization term was not included because energy minimization would then give unexpected results. Figure III-4 shows the result of minimizing the energy after initializing a domain wall, demagnetization included. It was only after applying a strong enough field to the strip that the domain wall would return back to its form perpendicular to the x-axis. A weaker field causes the magnetic domains to reflect over themselves. The remainder of our results in this section will be obtained without including demagnetization.

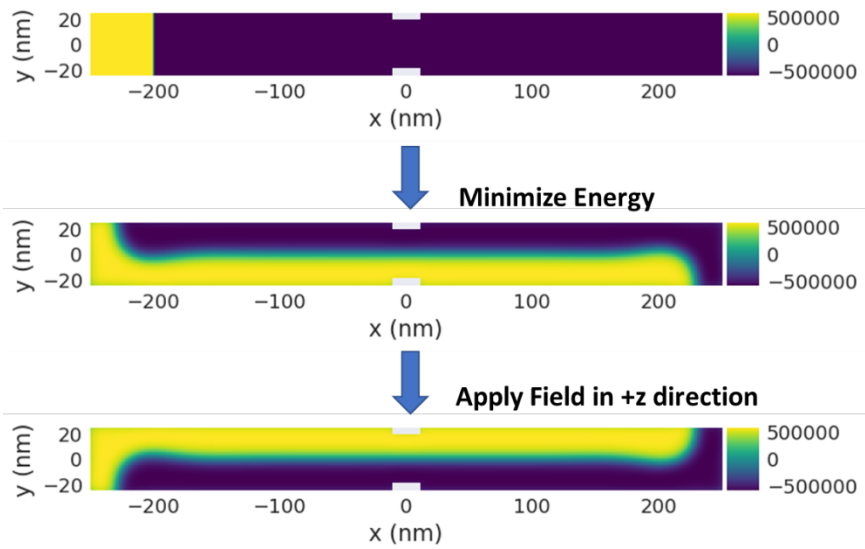

Figure III-4: The results when including the demagnetization term in the energy equation. The applied field interacts with the stray fields in a way which causes the domains to reflect over themselves.

Does the minimum field strength needed to drive the wall across the film change if we first pin the wall to the notches? We first apply a field just strong enough to move the wall to the notches. Then, we apply a new field without resetting the magnetization to see what minimum field is now needed to reach the end of the strip. Trial and error found that the minimum field is *still* $H = 1.16515 * 10^5$ A/m (Fig. III-5). A possible explanation for this result is that the notches in the strip create a local minimum in the energy landscape of the system at that location. The domain wall requires a minimum strength of magnetic field to crest this energy barrier and unpin itself, like how rolling a ball up a hill requires a minimum energy to do so. Therefore, whether or not the wall starts before this local minimum or within it does not matter, the same energy is needed to move the wall past the notches and across the strip.

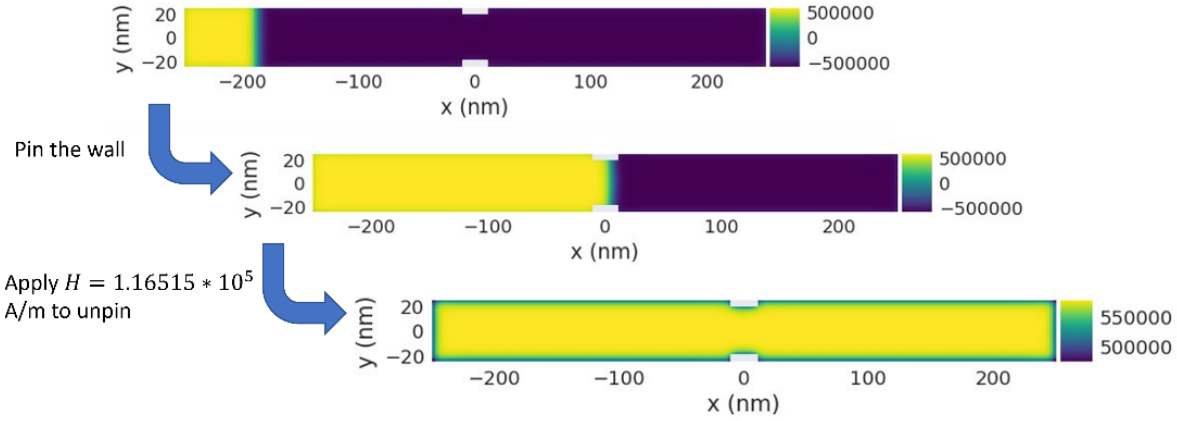

*Figure III-5: We start with the minimized energy domain wall (top figure). A field is applied to the domain wall which is just enough to pin it to the notches (middle figure). Finally, trial and error revealed that the same field H = 1.16515 * 10^5 A/m is required to drive the wall across the film despite first being pinned (bottom figure).*

When a field is applied to the wall which is almost strong enough to move it past the notches, the domain wall can be seen warping as it stretches beyond the defects which pin it.

However, when the field is then removed and the system is minimized again, the wall moves back to the center of the notches, as seen in Fig. III-6. This is like if you were to release a ball close to the top of a hill; the ball will roll back down to the lowest point, or the local minimum of energy. Additionally, it appears that there are other minima located across the strip besides the one found at the notches, with one shown in Fig. III-7. The physical origin of these minima remains unknown to us, but the notches do not seem to be the source because these other minima are still present even when the notches are filled in.

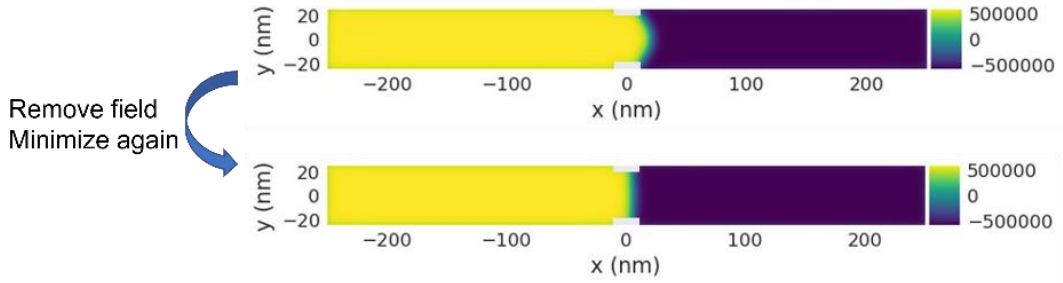

Figure III-6: A field is applied to the wall to almost unpin it from the notch entirely (top figure). Then the field is removed and energy is minimized again, causing the wall to move back to the center of the notches (bottom figure).

Figure III-7: An additional local minimum found along the strip. First, a field is applied to move the wall close to the end of the strip (top figure). Then, the field is removed and energy is minimized again, causing the wall to move into the local energy minimum (bottom figure).

Our next goal is to find the minimum field needed to move the wall across the strip for different notch depths. At additional depths of 10 nm, 15 nm, and 20 nm, we found minimum fields of $1.2238 * 10^5$A/m, $1.52643 * 10^5$A/m, and $2.7313 * 10^5$A/m, respectively. We also found that in each case the minimum field would not change based on if the wall was first pinned to the notches, consistent with what we found for the 5 nm depth notches.

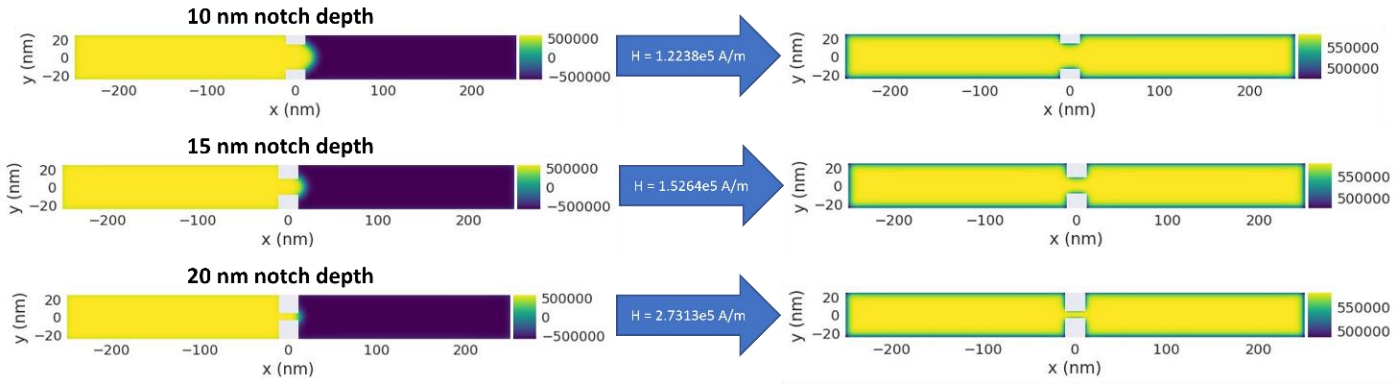

Figure III-8: Minimum field strength necessary to move the wall across a magnetic strip with 10 nm depth notches (top figures), 15 nm depth notches (middle figures), and 20 nm depth notches (bottom figures).

With these results we can construct a relationship between notch depth and the minimum field strength needed to drive the wall across the strip. Working with python fitting functions and some trial and error, we found that the minimum field strength seems to increase exponentially with a linear increase in notch depth. The relationship is given by the equation $y = a * Exp(b * t) + c$, where y is the minimum field needed, t is the notch depth, and a, b, and c are each constants given by 549.12, 0.2835, and 113759, respectively. The simulated data and fit are plotted in Fig. III-9.

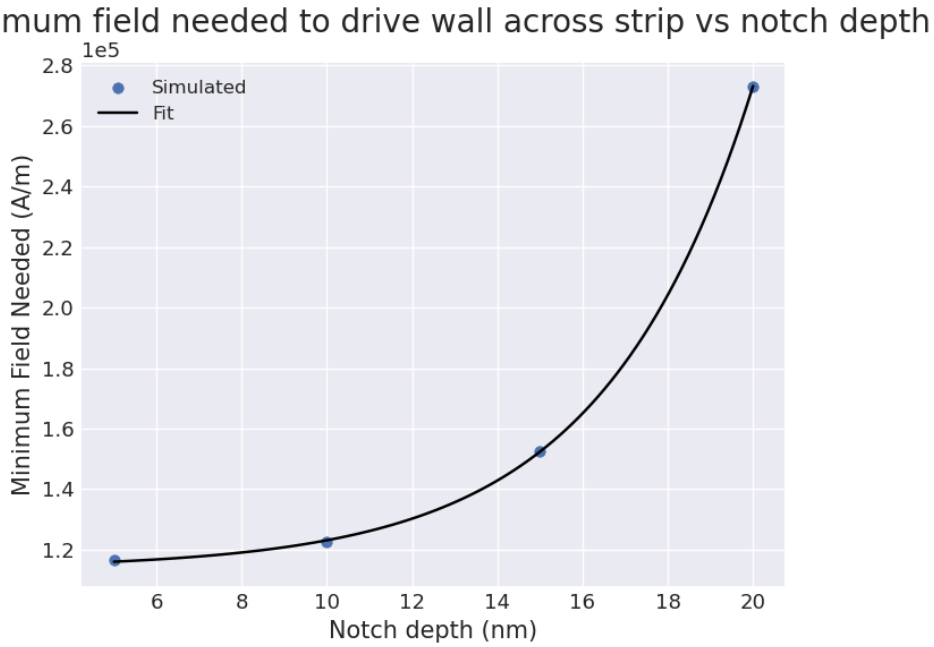

Figure III-9: Minimum field strength needed to drive wall all the way across film vs notch depth. The results found by Ubermag simulation are shown by blue dots, while the fit is given by the black line.

Conclusion:

Here we have explored the simulation of domain walls under both static and dynamic conditions using Ubermag. In initializing and relaxing the domains of a rectangular, thin film system under static conditions, we have observed directly the effects of anisotropy on the widths of the domain walls and demonstrated the necessity of anisotropy in stabilizing out-of-plane domain orientations. Additionally, we have observed that the inclusion the Dzyaloshinkii-Moriya interactions (DMI) enables coherent rotation of the moments in the domain wall region without needing additional initial domains. Finally, the first portion of the project concludes by noting that the demagnetization energy must be neglected in order to initialize domains at arbitrary locations that do not relax back to the center of the system, which is relevant to the later sections of the project.

We've demonstrated that the motions of domain walls can be effectively controlled using both an applied current and an applied field. Depending on the exact parameters of the field/current, the average domain wall velocity can be controlled. For the parameters simulated, we showed that a spin polarized current can move domain walls faster and in a more controlled fashion when compared to an applied field. We also demonstrated the effects of Walker breakdown in the presence of an axially applied magnetic field. Future work on the front of domain wall dynamics could include studying the effects of geometry on STT induced motion as well as Walker breakdown due to other mechanisms of motion.

Variations in a bulk material's anisotropy and exchange interactions can alter the motion of domain walls. When notches are created on a thin film, the energy landscape of the strip is changed. Minima in total energy based on domain wall position can be found at the locations of void defects. It was found that a minimum field strength applied to the film is needed in order to move a domain wall past these notches. If the minimum requirement is not met, the wall will be pinned to the notches, stuck at the bottom of an energy potential well. Additionally, larger (deeper) notches will pin the wall more easily. The minimum field strength appears to increase exponentially with a linear increase in notch depth. Future work could include calculations within Ubermag of the actual energy landscape of the magnetic strip. This could help us identify the origin of the extra minima found. Additionally, more time could be spent trying to understand the results obtained when including the demagnetization term during domain wall motion and pinning.